OCEAN CHEMISTRY

10.1126/sciadv.1500531

Effects of ocean acidification on marine dissolved organic matter are not detectable over the succession of phytoplankton blooms

Maren Zark,[1]* Ulf Riebesell,[2] Thorsten Dittmar[1]

Marine dissolved organic matter (DOM) is one of the largest active organic carbon reservoirs on Earth, and changes in its pool size or composition could have a major impact on the global carbon cycle. Ocean acidification is a potential driver for these changes because it influences marine primary production and heterotrophic respiration. We simulated ocean acidification as expected for a "business-as-usual" emission scenario in the year 2100 in an unprecedented long-term mesocosm study. The large-scale experiments (50 m^3 each) covered a full seasonal cycle of marine production in a Swedish Fjord. Five mesocosms were artificially enriched in CO_2 to the partial pressure expected in the year 2100 (900 µatm), and five more served as controls (400 µatm). We applied ultrahigh-resolution mass spectrometry to monitor the succession of 7360 distinct DOM formulae over the course of the experiment. Plankton blooms had a clear effect on DOM concentration and molecular composition. This succession was reproducible across all 10 mesocosms, independent of CO_2 treatment. In contrast to the temporal trend, there were no significant differences in DOM concentration and composition between present-day and year 2100 CO_2 levels at any time point of the experiment. On the basis of our results, ocean acidification alone is unlikely to affect the seasonal accumulation of DOM in productive coastal environments.

INTRODUCTION

About half of the CO_2 emitted to the atmosphere by human fossil-fuel burning since preindustrial times has been absorbed by the oceans (*1*), causing a continuous decrease in seawater pH by about 0.3 unit before the end of the 20th century (*2*). This rapid change in seawater chemistry has a potential impact on the future marine biogeochemical carbon cycle (*2*, *3*) through changes in marine primary production (*4*, *5*) and heterotrophic respiration (*6*, *7*). Marine dissolved organic matter (DOM) represents the largest active organic carbon pool within this cycle (~700 Gt) (*8*). Changes in pool size or reactivity would affect the long-term carbon storage capability of the ocean's interior. However, the impact of ocean acidification on the marine DOM pool remains unknown, particularly on its molecular composition and long-term reactivity (*9*–*12*).

A large fraction of oceanic net primary production is transferred to the DOM pool and respired to CO_2 via the microbial loop (*13*, *14*). However, a subset of DOM is highly persistent against microbial degradation and resides in the deep ocean on time scales of hundreds to ten thousands of years (*8*, *15*). The driving forces behind this recalcitrance are unknown (*16*), but most likely microbial processes govern the generation and transformation of recalcitrant DOM (*17*–*20*). The recalcitrant fraction of DOM represents by far the largest proportion and is thus the most important in terms of carbon storage (*21*).

Ocean acidification may stimulate microbial degradation of DOM (*6*, *7*). Therefore, it could induce lower carbon sequestration rates in the future ocean (*22*, *23*). However, the concurrent stimulation of DOM production (*9*, *11*) may offset the enhanced turnover, and the net effect of ocean acidification on bulk dissolved organic carbon (DOC) concentration may be insignificant on the short term (*10*, *12*, *24*). However, DOM is a highly complex mixture of presumably millions of different compounds (*16*). Changes on the molecular level can bring about differences in reactivity and long-term accumulation of DOM in the ocean that are not detectable on the bulk concentration level in short-term experiments.

To investigate the effects of ocean acidification on the molecular composition of the marine DOM pool, we conducted a unique long-term mesocosm study in the Gullmar Fjord in Sweden. Ten mesocosm units, each enclosing volumes of 50 m^3, were used to monitor a natural plankton community in situ under P_{CO_2} (partial pressure of CO_2) levels projected for the end of this century. Five of these mesocosms were artificially enriched in CO_2 to the partial pressure expected in the year 2100 (900 µatm) (*25*), and the other five served as controls (400 µatm). This experiment is unprecedented in terms of size and duration. We allowed for an extended acclimation time before the first algal bloom and monitored the full productive season over a time period at least twice as long as in any previous study.

We periodically monitored the DOM pool over the entire study through bulk DOC and total dissolved nitrogen (TDN) determinations as well as on a detailed molecular level through ultrahigh-resolution mass spectrometry [Fourier-transform ion cyclotron resonance mass spectrometry (FT-ICR-MS)]. With this technique, the diversity of DOM can be resolved on a molecular formula level, and as such, FT-ICR-MS is unprecedented in providing detailed molecular insights into the composition of DOM. The many thousands of different molecular masses that can be resolved by FT-ICR-MS (*26*, *27*) show a distinct succession over the course of phytoplankton blooms (*20*), and the technique is therefore well suited to obtain a very holistic overview of molecular DOM composition over the course of our experiments. As with any analytical technique, FT-ICR-MS has a defined analytical window, and

[1]Institute for Chemistry and Biology of the Marine Environment (ICBM), Research Group for Marine Geochemistry (ICBM-MPI Bridging Group), Carl von Ossietzky University of Oldenburg, Carl-von-Ossietzky-Straße 9-11, 26129 Oldenburg, Germany. [2]GEOMAR Helmholtz Centre for Ocean Research Kiel, Düsternbrooker Weg 20, 24105 Kiel, Germany.
*Corresponding author. E-mail: maren.zark@uni-oldenburg.de

compounds of low molecular mass (<150 daltons) and colloidal matter are outside of this window. Furthermore, highly labile compounds cycling on time scales of days were not targets by our sampling frequency and analytical techniques. Our experimental setup was intended to capture compounds that are produced in bloom situations (*20*) and turned over on time scales of weeks to months and longer. This component of DOM is of highest importance in the context of carbon sequestration.

RESULTS

General description of the mesocosms and bulk parameters

All 10 mesocosms exhibited a markedly reproducible succession of phytoplankton blooms and associated DOM production and consumption. Two sequential phytoplankton blooms were observed during the course of the experiment. The first bloom was sustained by inorganic nutrients and peaked around day 31 with an average chlorophyll *a* concentration of 6.8 µg liter^{-1} (Fig. 1A). TDN at the beginning of the study represented the combined concentrations of dissolved inorganic nitrogen (DIN) and dissolved organic nitrogen (DON) (Fig. 1B). DOC concentrations almost doubled from 149 ± 11 µM on day −1, the day before the first CO_2 addition, to 256 ± 38 µM on day 47 (mean ± SD, n = 10) (Fig. 1C) because of new production. The level is typical for the Gullmar Fjord at this time of the year (*28*). Inorganic nitrogen was consumed during this first bloom phase, and TDN then was constituted only by DON. The second bloom was fueled by the recycling of elements from organic matter and occurred around day 53 with a lower chlorophyll *a* maximum of 4.3 µg liter^{-1} (Fig. 1A). During recycled production, DOC concentrations decreased to a minimum of 149 ± 6 µM close to the end of the study. DOC/DON molar ratios started well above the classical Redfield ratio of 6.6, with decreasing values until the onset of the first phytoplankton bloom on day 20 (Fig. 1D). Superimposed onto these broad coherent trends, DOC concentrations consistently fluctuated from day to day in all 10 mesocosms. These irregular fluctuations are partly due to analytical uncertainty, which is inherent to bulk DOC analysis under such complex experimental settings. Most importantly, there was no statistically significant difference ($P < 0.01$) between the CO_2 treatments for all time points for chlorophyll *a*, DOC, DON, and TDN concentrations. The only exception was one sampling day (day 53), where TDN concentrations

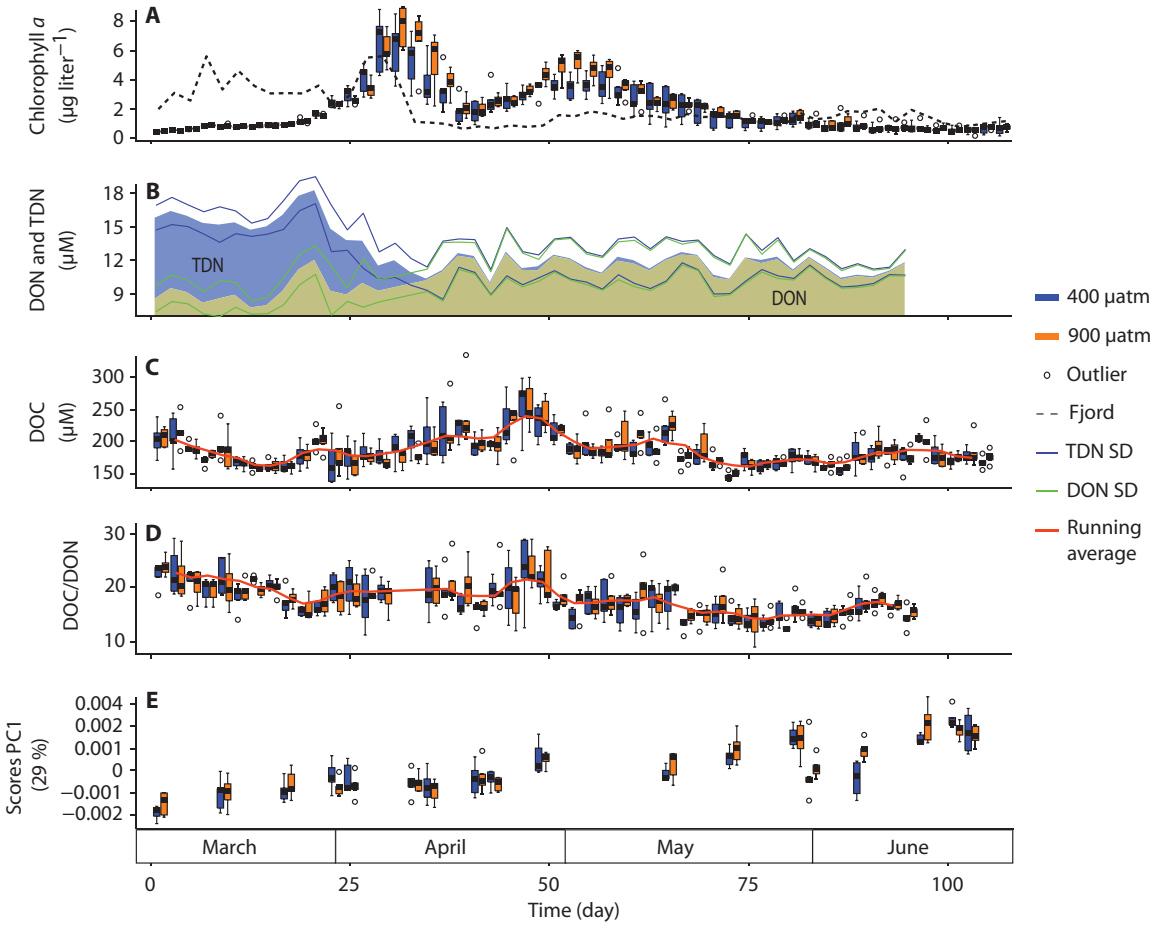

Fig. 1. Time series of bulk and molecular data of the 10 mesocosms. Box plots include median, SD, maximum and minimum values, and outliers. Orange boxes are for the five mesocosms with high PCO_2; blue boxes are for the five control mesocosms. Dotted time series are for Gullmar Fjord ambient water. (**A**) Chlorophyll *a* concentration. (**B**) TDN and DON concentrations, displayed as average values for all 10 mesocosms. (**C**) DOC concentration. (**D**) DOC/DON molar ratio. (**E**) Results from the PCA (PC1) of 7360 molecular formulae and their MS signal intensities.

were apparently different between the two CO_2 treatments. On a lower significance level ($P < 0.05$), there were only up to 4 days that showed differences for chlorophyll *a* (days 3, 49, 51, and 53), DOC (days 33, 61, and 73), DON (days −1, 53, and 79), and TDN (day 53) concentrations. These apparent differences did not show a consistent trend over time or between parameters. When considering several hypotheses in the same test, the problem of multiplicity arises (*29*). If one accounts for this family-wise error rate, for example, with the Holm-Bonferroni correction (*29*), none of the apparent differences between CO_2 treatments is significant at any meaningful significance level.

DOM molecular composition

A total of 11644 resolved masses of singly charged, intact compounds were detected with FT-ICR-MS (Fig. 2). Signal intensities followed a bell-shaped distribution along the mass axis with a weighted arithmetic mean of 391 ± 4 daltons (average and SD for all samples). This overall pattern was the same for all samples, but individual masses differed among samples with respect to their presence and signal intensity. For multivariate statistical analysis, the same number (7360) of the most intense detected masses was considered for each sample.

Using principal components analysis (PCA), we were able to summarize 29% of the total variability of the complex molecular information in a single component (PC1). This component showed a highly reproducible trend among the 10 independent mesocosm units over time (Fig. 1E). A Pearson correlation of the components from PCA with the environmental data revealed that PC1 was inversely correlated with chlorophyll *a* concentration ($P < 0.01$) but not with PCO_2 treatment (Table 1). A positive correlation of PC1 was observed with SiO_4^{4-}, PO_4^{3-}, NO_2^-, and NO_3^- concentrations ($P < 0.001$). However, none of the first 10 principal components pointed toward an influence of CO_2 manipulation. By comparing the distances to the respective group centroid (PerMANOVA), we obtained the same result, because there were no significant differences in the molecular data for samples from CO_2-enriched compared to control mesocosms.

Individual molecular formula analysis of the relative signal intensities of the 5 replicate mesocosms showed similar results. Multiple Student's *t* tests were individually performed for each PCO_2 treatment at each time point, revealing an increasing number of molecular formulae that significantly ($P < 0.001$) differed from the starting conditions over time. In total, up to 16% of the considered molecular features showed a variation between day −1 and the last day of sampling (Fig. 3), which is the result of specific molecules being released or used by the resident microbial communities inside the mesocosms. We performed the same test for the molecular formulae from the different PCO_2 treatments. We observed only a small number of formulae that significantly differed, ranging only from 0 to 20 formulae for all time points (Fig. 4). The abovementioned family-wise error rate is of major relevance to our family of 7360 tests (molecular formulae). To compare our results with what random chance might produce (*30*), we generated artificial data sets of 7360 randomly generated numbers. Comparison of two random data sets showed a similar number of apparent differences to that observed between two CO_2 treatments (Figs. 3B and 4B). Hence, CO_2 levels did not affect the net molecular composition of the DOM pool covered by our analysis after a succession of phytoplankton blooms. This consistency among the mesocosms is striking, given the fact that in 5 of 10 mesocosms, PCO_2 was more than doubled, and that 7360 independent molecular features were considered of which >1000 showed a consistent succession over time.

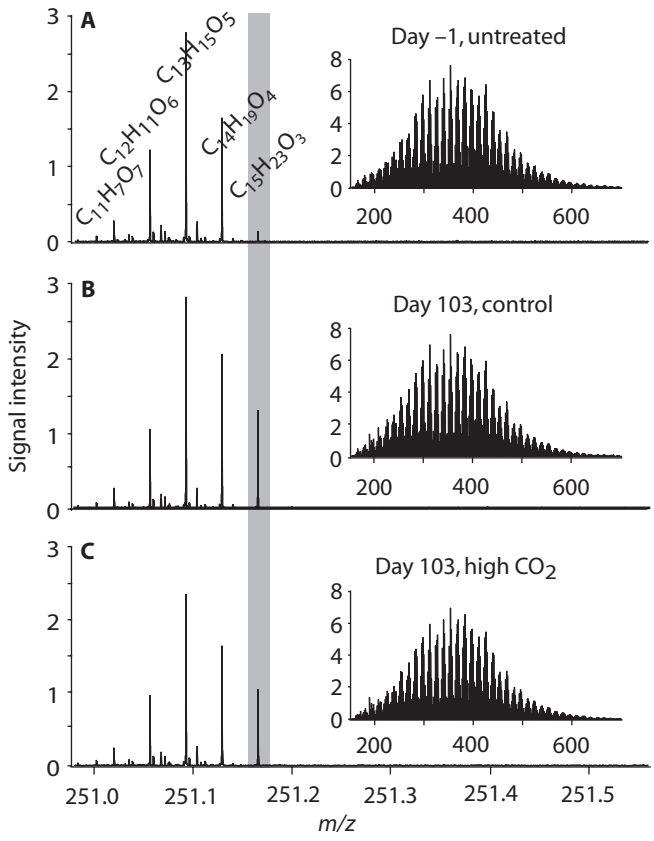

Fig. 2. Examples of FT-ICR-MS spectra of mesocosm DOM at different time points and with different treatments. (**A**) Day −1 after closing mesocosm bags. (**B**) Day 103 ambient PCO_2 mesocosm. (**C**) Day 103 high PCO_2 mesocosm. Mass range is from 150 to 750 daltons and zoomed into one exemplary nominal mass (251 daltons). *m/z*, mass/charge ratio. The peak in the gray shaded area is exemplary of mass peaks that show a significant difference in intensities between day 1 and day 103 in a Student's *t* test ($P < 0.001$).

Table 1. Pearson correlation of environmental parameters with the PCA scores. Significant correlations are noted by the level of significance (*P* value); "—" denotes absence of any detectable correlation ($P > 0.05$).

	PC1 (25%)	PC2 (17%)
CO_2	—	—
DOC	—	—
NO_2^-/NO_3^-	3.07×10^{-9}	2.39×10^{-4}
PO_4^{3-}	2.09×10^{-9}	6.54×10^{-5}
SiO_4^{4-}	1.71×10^{-9}	3.38×10^{-5}
NH_4^+	—	3.49×10^{-2}
Chlorophyll *a*	6.25×10^{-3}	—

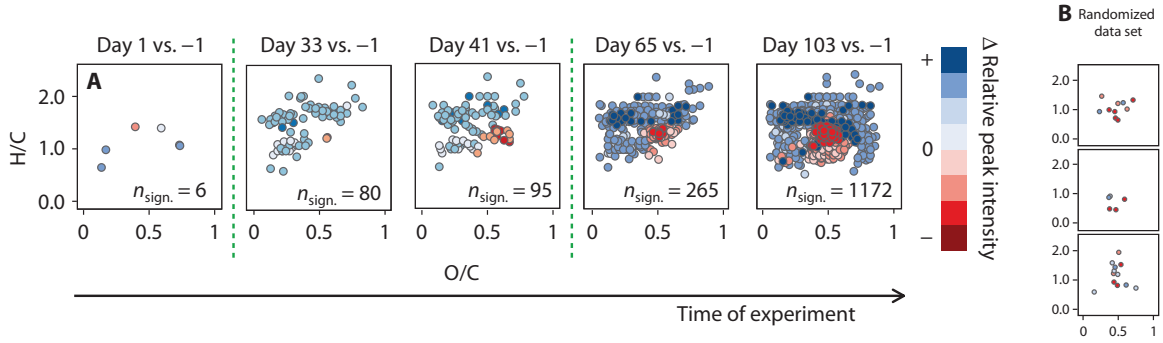

Fig. 3. Molecular differences over time. (**A**) Exemplary van Krevelen diagrams showing only the molecular formulae (out of 7360) that significantly varied in their intensities over the course of the experiment compared to day −1 for all 10 mesocosm replicates ($P < 0.001$). The different colors represent differences in normalized relative peak intensity: blue dots indicate an increase in peak intensities, whereas red dots indicate a decrease in peak intensity. Green dashed lines represent time points of phytoplankton blooms. (**B**) The results are within the statistical error, determined by performing the same test on a randomized data set.

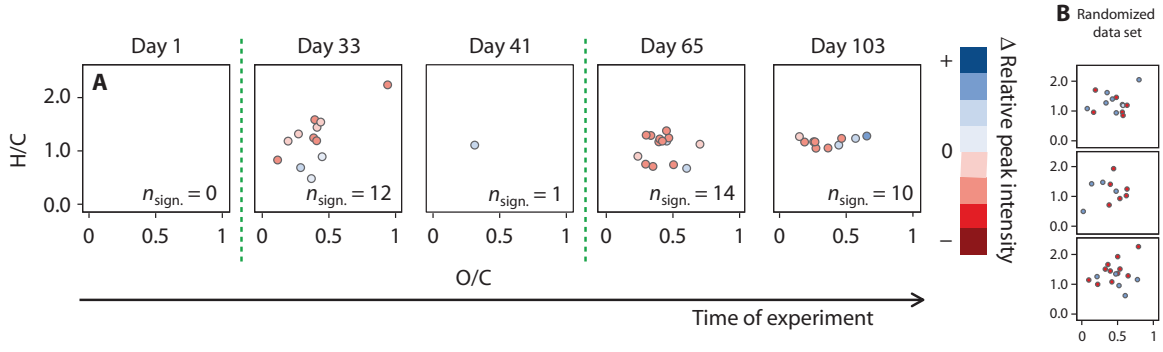

Fig. 4. Molecular differences between different CO_2 treatments. (**A**) Exemplary van Krevelen diagrams showing only the molecular formulae (out of 7360) that significantly varied in their intensities between the five high PCO_2 and control mesocosm replicates, tested for the respective day ($P < 0.001$). The different colors represent differences in normalized relative peak intensity: blue dots indicate an increase in peak intensity, whereas red dots indicate a decrease in peak intensity. Green dashed lines represent time points of phytoplankton blooms. (**B**) The results are within the statistical error, determined by performing the same test on a randomized data set.

DISCUSSION

At first view, our results seem to contradict some previous observations. In a similar (though much shorter) experiment in Svalbard, elevated PCO_2 conditions enhanced primary production (*9*), and an associated accumulation of DOC was indirectly calculated with a budget approach (*11*). These results were interpreted as evidence for enhanced DOC production and accumulation under high PCO_2 conditions (*31*). However, bacterial and extracellular enzyme activities were also stimulated in this (*32*) and other (*6*, *33*) studies, which may have enhanced the turnover of DOM. Consistent with this explanation, in a different mesocosm study in Norway (*34*), bacterial abundance was 28% higher in CO_2-manipulated mesocosms compared to controls, and DOC concentrations did not differ between treatments, even though PCO_2 levels in this experiment exceeded three times those in our approach. In other experiments, no differences were observed for DOC and DON concentrations under ocean acidification conditions (*10*, *12*, *24*). The apparent contradiction between the study in Svalbard (*31*) and most other studies may possibly be due to a hidden pool of very quickly cycling DOM compounds that were turned over on short time scales (*9*, *11*) and were not resolved by the sampling scheme applied in most studies, including ours. Enhanced production is likely closely coupled to removal of DOM components. Thus, ocean acidification may not have a detectable effect on the concentration of the most labile compounds, because enhanced production is quickly counteracted by stimulated consumption. Aggregation of polysaccharide-rich particles such as transparent exopolymer particles (TEP) may be another mechanism for fast removal of excess freshly produced DOM (*10*).

More importantly, in the context of our study, CO_2-induced changes in the quick cycling of labile DOM, if present, did not affect the composition of the remaining DOM pool after a phytoplankton bloom phase. This may not be surprising, considering the long turnover times of some of the components, but small-scale mesocosm experiments have provided evidence that compounds that are molecularly undistinguishable from the most refractory DOM in the deep ocean can be produced via microbial activity within months (*20*). Together, our findings are consistent with the scenario that ocean acidification has an insignificant impact on DOM that is turned over on time scales of weeks to months and longer. This component of DOM is of highest importance in the context of carbon sequestration because it has the potential to accumulate in the global ocean over historic time scales. Elevated PCO_2 levels did not affect the molecular composition of DOM despite a clear succession of molecular composition over time in response to

microbial activity. This finding suggests that elevated PCO_2 levels have no major impact on the composition of DOM in a coastal setting through changes in the functioning of the microbial loop.

One major difference in the experimental design from previous mesocosm studies is that, in our study, the community had more time to acclimate to elevated PCO_2 before the seasonal increase in primary production. This possibly allowed the microbial community to establish a balance between DOM production and consumption, which may not have been achieved in earlier studies. This is supported by the fact that most coastal environments naturally exhibit fluctuations in PCO_2. The Gullmar Fjord is no exception. Furthermore, responses to the relatively moderate levels of PCO_2 that were chosen for our study could simply be too small to be detected.

In the most productive areas of the world oceans, the assimilation and release of CO_2 by planktonic communities causes a natural fluctuation of seawater pH on short time scales to which microbial communities are adapted. Our results indicate that microbial communities may also be resilient to gradual changes in seawater pH as predicted for the next century, at least with respect to the concentration and molecular composition of seasonally accumulated DOM. Overall, the results of our study strongly support the scenario that ocean acidification alone will not change the amount of coastal net primary production that is funneled into the recalcitrant DOM pool via microbial activity.

MATERIALS AND METHODS

Experimental setup

The mesocosm study was performed between 8 March and 24 June 2013 (109 days) at the University of Gothenburg Sven Lovén Centre for Marine Sciences in Kristineberg, Sweden. Ten cylindrical Kiel Off-Shore Mesocosms for Future Ocean Simulations (KOSMOS) were deployed in the Gullmar Fjord at 58°16′N 11°29′E. Water depth at this site was about 50 m, and the average water temperature increased from 0.5°C in March to 16°C in June. The mesocosms consisted of floating frames with attached polyurethane bags of about 50-m^3 volume, 2-m diameter, and 17-m water depth. All bags were filled at the same time with seawater from the fjord, which was passed through a 3-mm net during filling to keep a natural plankton community, but excluding larger organisms. The average salinity was 29.3 inside the mesocosms. Details about the technical features and experimental setup of the KOSMOS are described by Riebesell *et al.* (*35*) and Schulz *et al.* (*36*). To simulate future ocean acidification conditions, 5 mesocosm replicates were manipulated to a target PCO_2 level of 900 µatm. The other 5 mesocosms were used as controls at ambient PCO_2 values of initially 400 µatm. The manipulation with carbon dioxide was done by stepwise addition of CO_2-saturated seawater. The pH ranged from 7.82 to 8.03 for the controls and from 7.46 to 7.85 for the enriched mesocosms. All mesocosms were open to the atmosphere, and thus, CO_2-enriched water had to be added at several time points to keep the PCO_2 level close to the target. The different treatments were randomly distributed over the mooring arrays. Mesocosm bags were frequently cleaned to avoid wall growth and to allow natural light penetration through the water column.

Sample preparation and bulk analysis

Representative samples of mesocosms and the surrounding fjord water were collected from boats every other day at 0900 to 1100 local time, starting from the day before the first CO_2 manipulation (day −1). We used 5-liter integrating water samplers (IWS; Hydrobios), giving a representative sample for the upper 15 m of the water column. pH was measured with a spectrophotometer (Agilent 8453) with 1-cm cuvettes at 25°C following the protocol of Clayton and Byrne (*37*). The data were corrected to in situ temperature and reported on the total pH scale. Chlorophyll *a* concentrations were determined by filtration of 250 to 500 ml of sample onto GF/F filters (0.7 µm, Whatman). The filters were stored at −80°C for 24 hours and homogenized in 90% acetone with glass beads in a cell mill. The centrifugate was analyzed fluorometrically for chlorophyll *a* (*38*).

For DOC and TDN analysis, samples were collected in duplicate and directly filtered from the IWS sampler via gravity filtration through 0.7-µm GF/F precombusted (400°C, 4 hours) glass microfiber filters (Whatman) into precombusted 20-ml glass vials with acid-rinsed Teflon caps (Wheaton). Immediately after filtration, the samples were acidified with HCl (25%, analysis grade, Carl Roth) to pH 2. DOC and TDN concentrations were analyzed using a high-temperature catalytic oxidation method (*39*) with a Shimadzu (Japan) TOC-VCPH/CPN Total Organic Carbon Analyzer, equipped with an ASI-V autosampler and a TNM-1 module for the determination of TDN. Measurement accuracy was controlled with the Deep Atlantic Seawater Reference material (DSR, D. A. Hansell, University of Miami, Miami, FL) for every run. The error for DOC and TDN analysis was, on average, 4 and 6%, respectively. To identify contaminated samples, we calculated the deviation between the replicates for each mesocosm every sampling day. If the DOC concentrations deviated by 30% or more between replicates, the one with higher DOC concentration was considered to be contaminated and excluded from the data set. The data were then pooled for control and high PCO_2 mesocosms and checked for outliers (Dixon-Dean test, $P < 0.05$). Average values were calculated for each mesocosm and time point from the remaining data. The same procedure was applied to the measured TDN concentrations. We calculated DON concentrations from TDN by subtracting the concentration of all DIN species from TDN. DIN is the sum of nitrate, nitrite, and ammonium concentrations that were measured using a segmented flow analyzer (SEAL QuAAtro). For graphical data presentation of chlorophyll *a*, DOC, and DOC/DON concentrations, values outside of 1.5 times the interquartile range above the upper and below the lower quartiles were displayed as outliers. A running average was calculated for DOC and DOC/DON concentrations by calculating the average of the combined values from the respective sampling day, the day before, and the day after.

Samples for molecular characterization were collected from the IWS sampler into 2-liter acid-rinsed polycarbonate bottles (Nalgene). The samples were transported to shore and stored at in situ water temperatures in the dark until processing on the same day. After filtration through 0.7-µm GF/F glass microfiber filters (Whatman) with manual vacuum pumps (<200 mbar), the samples were acidified with HCl (25%, analysis grade, Carl Roth) to pH 2. Samples were stored at 4°C in the dark. The samples were extracted by solid-phase extraction (SPE) following the protocol of Dittmar *et al.* (*40*). We used a commercially available modified styrene divinylbenzene polymer resin (PPL, 1 g, Agilent). Before use, the cartridges were soaked in methanol [high-performance liquid chromatography (HPLC) grade, Sigma-Aldrich] overnight and sequentially rinsed with methanol and 0.01 M HCl in ultrapure water. After being loaded onto the cartridges, the samples were rinsed with 0.01 M HCl to remove remaining salts and dried with nitrogen gas (analysis grade, Air Liquide). The extracted DOM was eluted with 6 ml of methanol and stored in precombusted glass vials at −20°C. To determine extraction efficiency, aliquots of the methanol extract were dried

and redissolved in ultrapure water. The average extraction efficiency was 45 ± 6% on a carbon basis. Especially colloidal matter and small ionic compounds may escape extraction and are likely lost from our analytical window. Procedural blanks were prepared by processing ultrapure water in the same way as the DOM samples. DOC concentrations in the resulting extracts were below the detection limit (*41*).

Molecular characterization

DOM consists of a multitude of compounds in very small concentrations, and thus, a separation of the single compounds surpasses the technical resolution of conventional analytical techniques (*42*–*44*). As a consequence, less than 7% of the compounds in DOM can be assigned to molecularly defined building blocks such as sugars and amino acids (*45*). Ultrahigh-resolution FT-ICR-MS has revolutionized the field of DOM research because it provides chemical information on thousands of individual molecules (*46*). More than tens of thousands of single compounds in DOM can be resolved in the mass spectra and assigned to molecular formulae owing to the ultrahigh mass accuracy and resolution (*26*, *27*).

MS analysis of SPE extracts was done with FT-ICR-MS on a 15-T Solarix system (Bruker Daltonics) equipped with an electrospray ionization source (ESI, Bruker Apollo II) applied in negative ionization mode. Methanol extracts were diluted with ultrapure water and methanol to give a final concentration of 20 mg C liter^{-1} in a 1:1 mixture of methanol (HPLC grade, Sigma-Aldrich) and ultrapure water. For each measurement, 500 scans were accumulated in a mass window of 150 to 2000 daltons. Spectra were internally calibrated with a reference mass list, using the Bruker Daltonics Data Analysis software package. The mass error of the calibration was <0.06 ppm for all samples. In addition to the exclusion criterion of a signal-to-noise (S/N) ratio of 4 or higher, small peaks with S/N ratios of <20 that occurred in less than 20% of the samples were also excluded. All 209 samples from a total of 19 time points (mesocosms and fjord samples) were analyzed by FT-ICR-MS in random order. Four samples were excluded from further data evaluation because of contaminations. To test the reproducibility and stability of the FT-ICR-MS analysis, we used DOM extract of North Equatorial Pacific Intermediate Water (NEqPIW) as in-house reference sample (*47*). We used MatLab routines developed by our working group for molecular formula assignment and further data processing. Only peaks with S/N ratios of 4 or higher that fulfilled the criteria stated by Koch *et al.* (*48*) were considered. All molecules were detected as singly charged ions. Molecular formulae were assigned to these masses according to the criteria set by Koch *et al.* (*48*) and Rossel *et al.* (*49*), with consideration of the elements C, H, O, N, S, and P. As with any analytical technique, FT-ICR-MS has its analytical detection window. The analytical settings were chosen to detect as many compounds as possible to obtain the most informative picture of DOM molecular composition. Nevertheless, the principle of FT-ICR-MS prevents the detection of very small compounds (<150 daltons) or colloidal matter.

Statistical analysis of FT-ICR-MS data

For multivariate statistical analyses, we considered the same number of detected masses for each sample. For this selection, the peak intensities were sorted in a ranked intensity order, independent for each sample, and the same number of masses with the most intense peaks was selected. Fjord samples were treated independently. The data were then normalized to the sum of peak intensities and finally used for statistical analysis. Variations in the molecular DOM composition were characterized by PCA. To identify links between the scores for the principal components and environmental parameters (type of CO_2 treatment and concentrations of chlorophyll *a*, ammonium, nitrate, nitrite, phosphate, silicate, and DOC), a second PCA was calculated from the data of time points, to which the respective environmental parameters were available. On this basis, a Pearson correlation (two-tailed) was done (fig. S1). Furthermore, we tested the data from both CO_2-enriched and control mesocosms over the entire time period by PerMANOVA (*50*). The average distance to each group centroid was calculated on the basis of a matrix of Euclidean distances. This distance was equivalent to the average distance among all pairwise group member combinations and served as a measure of dispersion. The differences in dispersions of both groups were then tested for significance by permutation. Furthermore, the intensities of the molecular formulae of both groups were tested for differences at each individual sampling time point as well as at the start of the study by a Student's *t* test ($P < 0.001$). Randomized data were generated in the intensity ranges of the peaks occurring in the analyzed spectra. All statistical analyses were done with the software package R (version 3.0.2, package "vegan") (*51*). The MS signal intensity of each detected molecular formula, as well as DOC and chlorophyll *a* concentrations and molar DOC/DON ratios of samples from CO_2-enriched and control mesocosms, was tested for differences by Student's *t* test.

SUPPLEMENTARY MATERIALS

Supplementary material for this article is available at http://advances.sciencemag.org/cgi/content/full/1/9/e1500531/DC1

Pearson correlation of environmental parameters

Fig. S1. Pearson correlation of environmental parameters with the scores of the principal components analysis.

REFERENCES AND NOTES

1. C. L. Sabine, R. A. Feely, N. Gruber, R. M. Key, K. Lee, J. L. Bullister, R. Wanninkhof, C. S. Wong, D. W. R. Wallace, B. Tilbrook, F. J. Millero, T.-H. Peng, A. Kozyr, T. Ono, A. F. Rios, The oceanic sink for anthropogenic CO_2. *Science* **305**, 367–371 (2004).
2. K. Caldeira, M. E. Wickett, Oceanography: Anthropogenic carbon and ocean pH. *Nature* **425**, 365 (2003).
3. U. Riebesell, A. Körtzinger, A. Oschlies, Sensitivities of marine carbon fluxes to ocean change. *Proc. Natl. Acad. Sci. U.S.A.* **106**, 20602–20609 (2009).
4. U. Riebesell, K. G. Schulz, R. G. J. Bellerby, M. Botros, P. Fritsche, M. Meyerhöfer, C. Neill, G. Nondal, A. Oschlies, J. Wohlers, E. Zöllner, Enhanced biological carbon consumption in a high CO_2 ocean. *Nature* **450**, 545–548 (2007).
5. R. G. J. Bellerby, K. G. Schulz, U. Riebesell, C. Neill, G. Nondal, E. Heegaard, T. Johannessen, K. R. Brown, Marine ecosystem community carbon and nutrient uptake stoichiometry under varying ocean acidification during the PeECE III experiment. *Biogeosciences* **5**, 1517–1527 (2008).
6. H.-P. Grossart, M. Allgaier, U. Passow, U. Riebesell, Testing the effect of CO_2 concentration on the dynamics of marine heterotrophic bacterioplankton. *Limnol. Oceanogr.* **51**, 1–11 (2006).
7. J. Piontek, M. Lunau, N. Händel, C. Borchard, M. Wurst, A. Engel, Acidification increases microbial polysaccharide degradation in the ocean. *Biogeosciences* **7**, 1615–1624 (2010).
8. D. A. Hansell, C. A. Carlson, D. J. Repeta, R. Schlitzer, Dissolved organic matter in the ocean: A controversy stimulates new insights. *Oceanography* **22**, 202–211 (2009).
9. A. Engel, C. Borchard, J. Piontek, K. G. Schulz, U. Riebesell, R. Bellerby, CO_2 increases ^{14}C primary production in an Arctic plankton community. *Biogeosciences* **10**, 1291–1308 (2013).
10. A. Engel, J. Piontek, H.-P. Grossart, U. Riebesell, K. G. Schulz, M. Sperling, Impact of CO_2 enrichment on organic matter dynamics during nutrient induced coastal phytoplankton blooms. *J. Plankton Res.* **36**, 641–657 (2014).
11. J. Czerny, K. G. Schulz, T. Boxhammer, R. G. J. Bellerby, J. Büdenbender, A. Engel, S. A. Krug, A. Ludwig, K. Nachtigall, G. Nondal, B. Niehoff, A. Silyakova, U. Riebesell, Implications of elevated CO_2 on pelagic carbon fluxes in an Arctic mesocosm study—An elemental mass balance approach. *Biogeosciences* **10**, 3109–3125 (2013).

12. G. A. MacGilchrist, T. Shi, T. Tyrell, S. Richier, C. M. Moore, C. Dumousseaud, E. P. Achterberg, Effects of enhanced pCO_2 levels on the production of dissolved organic carbon and transparent exopolymer particles in short-term bioassay experiments. *Biogeosciences* **11**, 3695–3706 (2014).
13. C. A. Carlson, P. A. Del Giorgio, G. J. Herndl, Microbes and the dissipation of energy and respiration: From cells to ecosystems. *Oceanography* **20**, 89–100 (2007).
14. P. A. del Giorgio, C. Duarte, Respiration in the open ocean. *Nature* **420**, 379–384 (2002).
15. D. A. Hansell, C. A. Carlson, Net community production of dissolved organic carbon. *Global Biogeochem. Cycles* **12**, 443–453 (1998).
16. T. Dittmar, in *The Biogeochemistry of Marine Dissolved Organic Matter*, D. A. Hansell, C. A. Carlson, Eds. (Elsevier Academic Press, Burlington, MA, ed. 2, 2015), pp. 369–388.
17. R. W. Eppley, B. J. Peterson, Particulate organic matter flux and planktonic new production in the deep ocean. *Nature* **282**, 677–680 (1979).
18. H. Ogawa, Y. Amagai, I. Koike, K. Kaiser, R. Benner, Production of refractory dissolved organic matter by bacteria. *Science* **292**, 917–920 (2001).
19. N. Jiao, G. J. Herndl, D. A. Hansell, R. Benner, G. Kattner, S. W. Wilhelm, D. L. Kirchman, M. G. Weinbauer, T. Luo, F. Chen, F. Azam, Microbial production of recalcitrant dissolved organic matter: Long-term carbon storage in the global ocean. *Nat. Rev. Microbiol.* **8**, 593–599 (2010).
20. H. Osterholz, J. Niggemann, H.-A. Giebel, M. Simon, T. Dittmar, Inefficient microbial production of refractory dissolved organic matter in the ocean. *Nat. Commun.* **6**, 7422 (2015).
21. D. A. Hansell, Recalcitrant dissolved organic carbon fractions. *Ann. Rev. Mar. Sci.* **5**, 421–445 (2013).
22. X. Mari, Does ocean acidification induce an upward flux of marine aggregates? *Biogeosciences* **5**, 1023–1031 (2008).
23. P. Schippers, M. Lürling, M. Scheffer, Increase of atmospheric CO_2 promotes phytoplankton productivity. *Ecol. Lett.* **7**, 446–451 (2004).
24. A. Engel, B. Delille, S. Jacquet, U. Riebesell, E. Rochelle-Newall, A. Terbrüggen, I. Zondervan, Transparent exopolymer particles and dissolved organic carbon production by *Emiliania huxleyi* exposed to different CO_2 concentrations: A mesocosm experiment. *Aquat. Microb. Ecol.* **34**, 93–104 (2004).
25. IPCC. *Climate Change 2013: The Physical Science Basis. Contribution of Working Group 1 to the Fifth Assessment Report of the Intergovernmental Panel on Climate Change*, T. F. Stocker, D. Qin, G.-K. Plattner, M. Tignor, S. K. Allen, J. Boschung, A. Nauels, Y. Xia, V. Bex, P. M. Midgley, Eds. (Cambridge Univ. Press, Cambridge, 2013), p. 1096.
26. B. P. Koch, M. Witt, R. Engbrodt, T. Dittmar, G. Kattner, Molecular formulae of marine and terrigenous dissolved organic matter detected by electrospray ionization Fourier transform ion cyclotron resonance mass spectrometry. *Geochim. Cosmochim. Acta* **69**, 3299–3308 (2005).
27. T. Dittmar, J. Paeng, A heat-induced molecular signature in marine dissolved organic matter. *Nat. Geosci.* **2**, 175–179 (2009).
28. A. M. Waite, Ö. Gustafsson, O. Lindahl, P. Tiselius, Linking ecosystem dynamics and biogeochemistry: Sinking fractionation of organic carbon in a Swedish fjord. *Limnol. Oceanogr.* **50**, 658–671 (2005).
29. S. Holm, A simple sequentially rejective multiple test procedure. *Scand. J. Stat.* **6**, 65–70 (1979).
30. R. Nuzzo, Scientific method: Statistical errors. *Nature* **506**, 150–152 (2014).
31. U. Riebesell, J.-P. Gattuso, T. F. Thingstad, J. J. Middelburg, Arctic ocean acidification: Pelagic ecosystem and biogeochemical responses during a mesocosm study. *Biogeosciences* **10**, 5619–5626 (2013).
32. J. Piontek, C. Borchard, M. Sperling, K. G. Schulz, U. Riebesell, A. Engel, Response of bacterioplankton activity in an Arctic fjord system to elevated pCO_2: Results from a mesocosm perturbation study. *Biogeosciences* **10**, 297–314 (2013).
33. S. Endres, J. Unger, N. Wannicke, M. Nausch, M. Voss, A. Engel, Response of *Nodularia spumigena* to pCO_2—Part 2: Exudation and extracellular enzyme activities. *Biogeosciences* **10**, 567–582 (2013).
34. S. Endres, L. Galgani, U. Riebesell, K.-G. Schulz, A. Engel, Stimulated bacterial growth under elevated pCO_2: Results from an off-shore mesocosm study. *PLOS One* **9**, e99228 (2014).
35. U. Riebesell, J. Czerny, K. von Bröckel, T. Boxhammer, J. Büdenbender, M. Deckelnick, M. Fischer, D. Hoffmann, S. A. Krug, U. Lentz, A. Ludwig, R. Muche, K. G. Schulz, Technical note: A mobile sea-going mesocosm system—New opportunities for ocean change research. *Biogeosciences* **10**, 1835–1847 (2013).
36. K. G. Schulz, R. G. J. Bellerby, C. P. D. Brussaard, J. Büdenbender, J. Czerny, A. Engel, M. Fischer, S. Koch-Klavsen, S. A. Krug, S. Lischka, A. Ludwig, M. Meyerhöfer, G. Nondal, A. Silyakova, A. Stuhr, U. Riebesell, Temporal biomass dynamics of an Arctic plankton bloom in response to increasing levels of atmospheric carbon dioxide. *Biogeosciences* **10**, 161–180 (2013).
37. T. D. Clayton, R. H. Byrne, Spectrophotometric seawater pH measurements: Total hydrogen ion concentration scale calibration of *m*-cresol purple and at-sea results. *Deep-Sea Res. Pt. I* **40**, 2115–2129 (1993).
38. N. A. Welschmeyer, Fluorometric analysis of chlorophyll *a* in the presence of chlorophyll *b* and pheopigments. *Limnol. Oceanogr.* **39**, 1985–1992 (1994).
39. J. Qian, K. Mopper, Automated high-performance, high-temperature combustion total organic carbon analyzer. *Anal. Chem.* **68**, 3090–3097 (1996).
40. T. Dittmar, B. Koch, N. Hertkorn, G. Kattner, A simple and efficient method for the solid-phase extraction of dissolved organic matter (SPE-DOM) from seawater. *Limnol. Oceanogr. Methods* **6**, 230–235 (2008).
41. A. Stubbins, T. Dittmar, Low volume quantification of dissolved organic carbon and dissolved nitrogen. *Limnol. Oceanogr. Methods* **10**, 347–352 (2012).
42. T. Dittmar, K. Whitehead, E. C. Minor, B. P. Koch, Tracing terrigenous dissolved organic matter and its photochemical decay in the ocean by using liquid chromatography/mass spectrometry. *Mar. Chem.* **107**, 378–387 (2007).
43. B. P. Koch, K.-U. Ludwichowski, G. Kattner, T. Dittmar, M. Witt, Advanced characterization of marine dissolved organic matter by combining reversed-phase liquid chromatography and FT-ICR-MS. *Mar. Chem.* **111**, 233–241 (2008).
44. G. C. Woods, M. J. Simpson, P. J. Koerner, A. Napoli, A. J. Simpson, HILIC-NMR: Toward the identification of individual molecular components in dissolved organic matter. *Environ. Sci. Technol.* **45**, 3880–3886 (2011).
45. K. Kaiser, R. Benner, Biochemical composition and size distribution of organic matter at the Pacific and Atlantic time-series stations. *Mar. Chem.* **113**, 63–77 (2009).
46. R. L. Sleigther, P. G. Hatcher, The application of electrospray ionization coupled to ultrahigh resolution mass spectrometry for the molecular characterization of natural organic matter. *J. Mass Spectrom.* **42**, 559–574 (2007).
47. N. W. Green, E. M. Perdue, G. R. Aiken, K. D. Butler, H. Chen, T. Dittmar, J. Niggemann, A. Stubbins, An intercomparison of three methods for the large-scale isolation of oceanic dissolved organic matter. *Mar. Chem.* **161**, 14–19 (2014).
48. B. P. Koch, T. Dittmar, M. Witt, G. Kattner, Fundamentals of molecular formula assignment to ultrahigh resolution mass data of natural organic matter. *Anal. Chem.* **79**, 1758–1763 (2007).
49. P. E. Rossel, A. V. Vähätalo, M. Witt, T. Dittmar, Molecular composition of dissolved organic matter from a wetland plant (*Juncus effusus*) after photochemical and microbial decomposition (1.25 yr): Common features with deep sea dissolved organic matter. *Org. Geochem.* **60**, 62–71 (2013).
50. M. J. Anderson, Distance-based tests for homogeneity of multivariate dispersions. *Biometrics* **62**, 245–253 (2006).
51. J. Oksanen, F. G. Blanchet, R. Kindt, P. Legendre, P. R. Minchin, R. B. O'Hara, G. L. Simpson, P. Solymos, M. H. H. Stevens, H. H. Wagner, Vegan: Community ecology package. R package version 2.0-10. http://CRAN.R-project.org/package=vegan (2013).

Acknowledgments: We thank the team of the Kristineberg mesocosm study in 2013 and particularly A. Ludwig for the logistical organization and coordination. We also thank the staff of the Sven Lovén Centre for Marine Sciences, University of Gothenburg, for hosting our team, and the captain and crew of R/V Alkor for support with transport and deployment of mesocosms. We thank S. Muellenmeister and I. Köster for help during sampling, and K. Klaproth, M. Friebe, and I. Ulber for technical support with FT-ICR-MS and DOC/TDN analysis. We also thank A. Ludwig for the analysis of chlorophyll *a* concentrations, and L. G. Anderson and Y. Ericson for the analysis of dissolved inorganic carbon and total alkalinity. Nutrient concentrations were provided by E. Achterberg, M. Esposito, and J. Bellworthy. We thank E. Achterberg for comments on the manuscript. **Funding:** Financial support for this study was provided by the German Ministry of Education and Research (BMBF, FKZ 03F0655D) through the BIOACID (Biological Impacts of Ocean ACIDification) project. Further financial support was provided by the Association of European Marine Biological Laboratories (ASSEMBLE, grant no. 227799) and the Heinz Neumüller Foundation. **Author contributions:** U.R. and T.D. designed the study. M.Z. and U.R. were involved with fieldwork. M.Z. analyzed samples and performed statistical data evaluation together with T.D. M.Z. wrote the paper, and all authors discussed the results and commented on the manuscript. **Competing interests:** The authors declare that they have no competing interests. **Data and materials availability:** DOC concentrations, TDN concentrations, and MS data are archived at the PANGAEA data library (doi:10.1594/PANGAEA.846137) and will be made available upon request.

Submitted 29 April 2015
Accepted 29 July 2015
Published 2 October 2015
10.1126/sciadv.1500531

Citation: M. Zark, U. Riebesell, T. Dittmar, Effects of ocean acidification on marine dissolved organic matter are not detectable over the succession of phytoplankton blooms. *Sci. Adv.* **1**, e1500531 (2015).

Effects of ocean acidification on marine dissolved organic matter are not detectable over the succession of phytoplankton blooms

Maren Zark, Ulf Riebesell and Thorsten Dittmar (October 2, 2015)

Sci Adv 2015, 1:.
doi: 10.1126/sciadv.1500531